Scientific Frontiers in Research on Extrasolar Planets
ASP Conference Series, Vol. 294, 2003
D. Deming and S. Seager, eds.

Rock Steady: The Challenges of a TPF Coronagraph

Charley Noecker

Ball Aerospace & Technologies Corp., P.O. Box 1062, Boulder, CO 80306

Abstract. NASA is investigating visible-light coronagraphs as a possible architecture for its Terrestrial Planet Finder (TPF) mission. To reach planets within 0.04–0.1 arcsec of their host stars, the primary mirror span must be roughly 10 meters; but to suppress the scattered starlight to match an earth-like planet, the wavefront must be corrected to better than an angstrom. That's the easy part. What's hard is holding it that way for hours. We will show that the challenging problem of planet finding can be met by a coronagraph. From a description of the design, operation, and the central trades and budgets, we will derive some of the more difficult technical requirements, motivating a separate discussion of technology development efforts (Kilston, in this conference).

1. Introduction

The challenge of detecting extrasolar planets is to achieve extremely high brightness contrast at small angles, since in visible light the total Earth-like planet flux is about 10^{-10} smaller than the star flux. (However, since the star flux mostly lands at a different place than the planet flux, the contrast is more like 3×10^{-7} at 5 Airy radii from the star in a standard circular diffraction pattern.) When observing nearby stars, planet-star separation angles can be as small as 40–80 milliarcseconds (mas), and as large as ≈ 1000 mas; this sets our goal for field-of-view.

The biggest issue in meeting these detection requirements is stray light, primarily stray starlight which reaches the planet location by two principal routes: diffraction from the aperture rim, and scatter from wavefront defects. Also important are stellar ghost images and stray sunlight, and local and exosolar zodiacal light. Zodi light is generally not an important source of background for an imaging system; thus a coronagraph approach is more robust to higher zodi levels and zodi clumps than is a mid-IR interferometric approach.

2. Nature of Noise Sources

Statistical photon noise sources, such as local and smooth exo-zodi, detector dark current, and stray sunlight, decrease in importance as the square root of the integration time. This could make possible picking out a faint planet against relatively large and smooth background (we call this case $Q << 1$, where Q is the ratio of planet counts to other counts at the same location). However, systematic error sources, such as residual diffracted light (after pupil/focal plane masks and the Lyot stop) or residual scattered light (after the DM and primary mirror actuators) won't average down, because they depend on vibrations and thermal effects, and are therefore time-variable. We have a strategic choice as to how much to limit the effect of time-variable backgrounds, and our team has chosen to require that the planet appear at least as bright as the background ($Q \sim 1$). As more is known about instrument variations, we will be able to refine this upper-level requirement

To achieve high Q values, our strategies for background noise reduction recognize that diffracted and scattered starlight are hard to discriminate from a planet in a single short exposure. Stray starlight must be kept constant enough to apply slower strategies. These can include (where appropriate): rotating the telescope around the line of sight to average out asymmetries, repeated measurements, and utilizing spectral information. Stray starlight must be low enough that shot noise in the background count rates doesn't drive integration times, and so heterodyne terms don't amplify the effects of time variations.

For planet detection at expected angular separations, we must control stray starlight especially at critical spatial frequencies, concentrating on the effects of wavefront ripples higher in frequency than the basic aberrations (focus, coma, spherical, trefoil, etc.), as well as on ripples longer-wave than surface roughness.

To summarize, detection of planets relies on maintaining low DC backgrounds at the planet location, as well as low variation in those DC backgrounds. Error budgeting must proceed on both of these fronts.

3. Coronagraph Approaches

The classical coronagraph approach employs a coronagraphic field occulter (CFO) located at a field stop; for highest performance, it uses a graded-attenuation spot (e.g., one with a gaussian profile; also see Kuchner & Traub). The spot blocks the central 3-5 Airy radii of the stellar image. Light escaping past the CFO edge is blocked by a subsequent Lyot stop at a re-imaged pupil; that annular mask works by scraping the outer parts of the beam at the image of the rim. Together these two barriers suppress ordinary aperture diffraction, although scatter from wavefront error still contributes and can dominate the stray light.

The shaped-pupil approach departs from circular symmetry in the entrance pupil to suppress diffraction in selected regions of the point-spread function (PSF). It also replaces the above CFO+Lyot combination with a different CFO shaped like the remaining stellar diffraction. For example, a square pupil has reduced diffraction along the image diagonals [ref Boeing-SVS team]. Novel pupil shapes developed by Spergel and Kasdin extend this idea to optimize the stellar rejection, with the mask shape alone sufficing to suppress diffraction to the required level (eliminating diffficult-to-manufacture graded-attenuation masks). An adjustably shaped pupil also might enable some amplitude correction. Figure 1 shows the near-ideal 2-segment design performance, using only an entrance pupil mask.

4. Features Of Optical System

The coronagraph's functional layout accommodates both classical and shaped-pupil approaches, which could be selectable on orbit. To accomplish the full TPF mission, an elliptical 10×4 m primary mirror provides maximal collecting area and a long dimension (to look close to the stars) within existing launch shrouds. The primary would be an unobscured off-axis segment surface of a parent optic of 11m diameter, f/1.5, preferably with a monolithic (one sheet) front surface to provide the best stray light control. If made of ULE/Zerodur or fused silica, it could be a meniscus, 4 cm thick, and lightweighted to 20–25 kg m^{-2}, mounted with control actuators to a graphite-cyanate backing structure (which adds $\sim$ 10 kg m^{-2}) for a total primary mirror mass of ≈ 940 kg.

Wavefront error (WFE) is the main concern, so in addition to the above actuators we assume that a deformable mirror (DM) will leave a minimum residual WFE in the pupil, with a white spectrum (PSD independent of spatial frequency). Then $\sigma < (N/8)\sqrt{\alpha C}$, where σ is the allowed RMS WFE within the spatial frequencies controllable by DM, N is the number of actuators across the DM width, α is the throughput factor due to pupil stops, and C is the ratio of integrated planet flux to (integrated star flux). With $N = 256$, 3 actuators/cycle, $\alpha = 0.5$, and $C = 10^{-10}$, at $\lambda = 500$ nm we get $\sigma \approx 75$ pm (spatial frequency range: 3–80 cycles/diameter) and a root-PSD of 0.8 pm m.

Layered control of WFE requires about 300 actuators on the primary mirror, covering the low spatial frequencies < 1.5 cycles/meter, or about 15 cycles/diameter. These actuators would have a stroke of tens of microns and a setting resolution of ~ 7 nm, to meet the DM stroke budget. The DM would have a stroke ~ 65 nm, and an element setting resolution ~ 0.05 nm.

Amplitude error compensation is vital, and phase correction (at the DM) can accomplish most of the correction. However, phase adjustments impose a bandwidth limitation, since amplitude error is mostly independent of λ, yet the phase correction scales as $1/\lambda$. Errors in the correction would then accumulate away from the center wavelength. If the amplitude error, $\delta A \sim 10^{-4}$ and the optical band full width $\delta\lambda/\lambda \sim 30\%$, the resulting leakage is

$$\frac{1}{12}\,(\delta A)^2 \left(\frac{\delta\lambda}{\lambda}\right)^2 = 7.5 \times 10^{-11}$$

which may be tolerable. To fully understand these effects, we need the amplitude PSD, but experimental data on this question are sparse at the required precision. Passive amplitude-error compensation would be a challenge for a 10-mirror system; we need better data to assess expected capability. Potentially an actuator (spatial light modulator) could make it easy, if it is achromatic, gentle on wavefront and polarization, and highly stable.

5. Steering Mirror vs. Body Pointing

The allowable telescope body-pointing error is based on the accumulation of WFE due to beam walk. In our simplified analysis of wavefront errors under rigid rotation of the telescope, repointing the telescope body leads to substantial

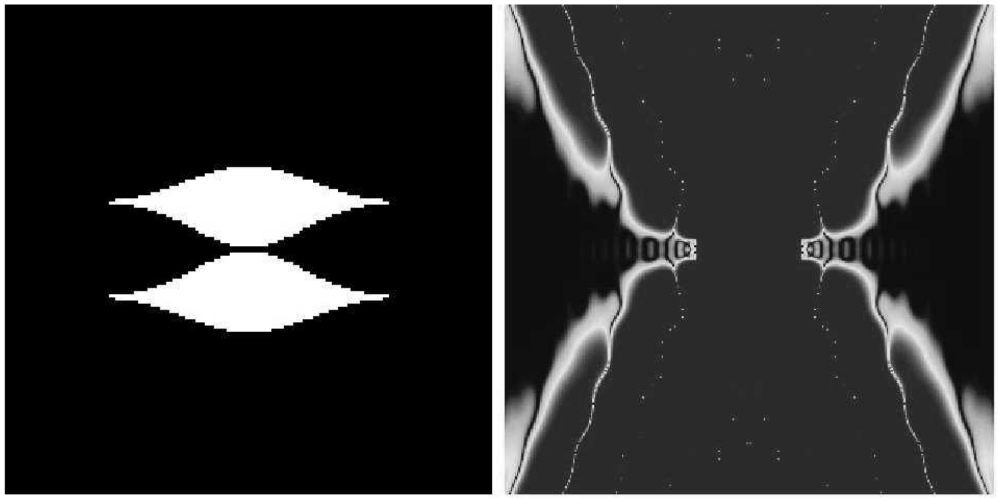

Figure 1. Spergel-Kasdin shaped pupil (left image), and the resulting diffraction pattern in the image plane.

beam walk across some mirrors, and using the FSM to maintain pointing on the CFO does not remove these errors. This beam walk changes the wavefront error contribution of those mirrors, so that the correction supplied by the DM moves sideways and is then incorrect for the new wavefront. Our estimate assumes the root-PSD for each mirror will be 10 times better than that measured nominally for the Hubble Space Telescope. Our result is that limiting body pointing error to 14 mas seems to control WFE to tolerable levels.

6. Conclusions

TPF coronagraph requirements are individually and collectively challenging, but within the grasp of a reasonable technology development effort, and the coronagraphic approach has some important advantages, if it proves technically feasible.

Acknowledgments. This work was performed for the Jet Propulsion Laboratory, California Institute of Technology, sponsored by the National Aeronautics and Space Administration, under Contract No. NAS7-1407.